# A Radical Mechanism in the Vanadium-Catalyzed Deoxydehydration of Glycols

Luis Carlos de Vicente Poutás,[†] Marta Castiñeira Reis,[†] Roberto Sanz,[‡] Carlos Silva López,[†] and Olalla Nieto Faza[*,¶]

[†]*Departamento de Química Orgánica. Facultad de Química. Universidade de Vigo. Campus Lagoas-Marcosende, 36310, Vigo, Spain*

[‡]*Departamento de Química. Facultad de Ciencias, Universidad de Burgos, Pza. Misael Bañuelos s/n, 09001 Burgos, Spain*

[¶]*Departamento de Química Orgánica. Facultade de Ciencias. Universidade de Vigo. Campus As Lagoas 32004, Ourense, Spain*

E-mail: faza@uvigo.es

Phone: +34 988 368 888

**Abstract**

We propose a novel mechanism for the deoxydehydration (DODH) reaction of glycols catalyzed by a $[Bu_4N][VO_2(dipic)]$ complex (dipic= pyridine-2,6-dicarboxylate) using triphenylphosphine as a reducing agent. Using density functional theory (DFT) we have confirmed that the preferred sequence of reaction steps involves reduction of the V(V) complex by phosphine, followed by condensation of the glycol into a [VO(dipic)(-O-$CH_2CH_2$-O-)] V(III) complex (**6**), which then evolves to the alkene product and the recovery of the catalyst. In contrast to the usually invoked closed-shell mechanism for the latter steps, where **6** suffers a [3+2] retrocycloaddition, we have found that the homolytic cleavage of one of the C–O bonds in **6** is preferred by 12 kcal/mol. The resulting diradical intermediate then collapses to a metallacycle which evolves to the product through an aromatic [2+2] retrocycloaddition. We use this key change in the mechanism to propose ways to design better catalysts for this transformation. The analysis of the mechanisms in both singlet and triplet potential energy surfaces, together with the location of the MECPs between them, showcase this reaction as an interesting example of two-state reactivity.

# Introduction

Biomass can become a viable and renewable alternative to the use of fossil oil as fuel or as a source of raw materials for the chemical industry. For this to happen however the products obtained from its processing, mainly polyalcohols, need to be transformed in other compounds that can be incorporated into the existing industrial processes. The most common approach involves deoxygenation or dehydration processes that reduce their content in oxygen, transforming them into more suitable industrial feedstocks. In this context, deoxydehydration (DODH) reactions have become appealing transformations because they preserve functionalization: a glycol yields an alkene, compared with hydrodeoxygenation (HDO) processes in which alkanes are obtained from alcohols. The first chemical approaches (as in opposed to biological alternatives to biomass valorization involving fermentations) rely on the use of heterogeneous catalysts that effect the hydrogenolysis of polyols. The most efficient among them use noble metals to activate hydrogen and tungsten or rhenium as additives,[1] but other systems such as Ni-Cu/$Al_2O_3$ have also been used.[2] Homogeneous reactions using rhenium catalysts, for which detailed mechanistic information (computational and experimental) is available,[3–15] are showing great potential in processes ranging from the deoxydehydration of glycols to the deoxygenation of epoxides, alcohols and carbonyl compounds, as does the derivatization of biomass polyols catalyzed by rhodium or iridium complexes.[16] The discovery of the activity of Mo(VI) and V(V) complexes, based on cheaper and more abundant metals, in the DODH of glycols[17–24] led us to focus on the study of the mechanism of these transformations. These complexes are versatile in terms of manipulation and derivatization, hence the goal is designing more efficient catalytic systems. In this work, we have studied the mechanism of the deoxydehydration of glycols to alkenes catalyzed by a [$Bu_4N$][$VO_2$(dipic)] complex (dipic= pyridine-2,6-dicarboxylate) using triphenylphosphine as a reducing agent described by Nicholas and Chapman in 2013.[20] The authors propose two alternative paths for this transformation, depending on the ordering of the steps involving the reduction of the catalyst with the phosphine and the coordination of the glycol to the

metal center (see Figure 1).

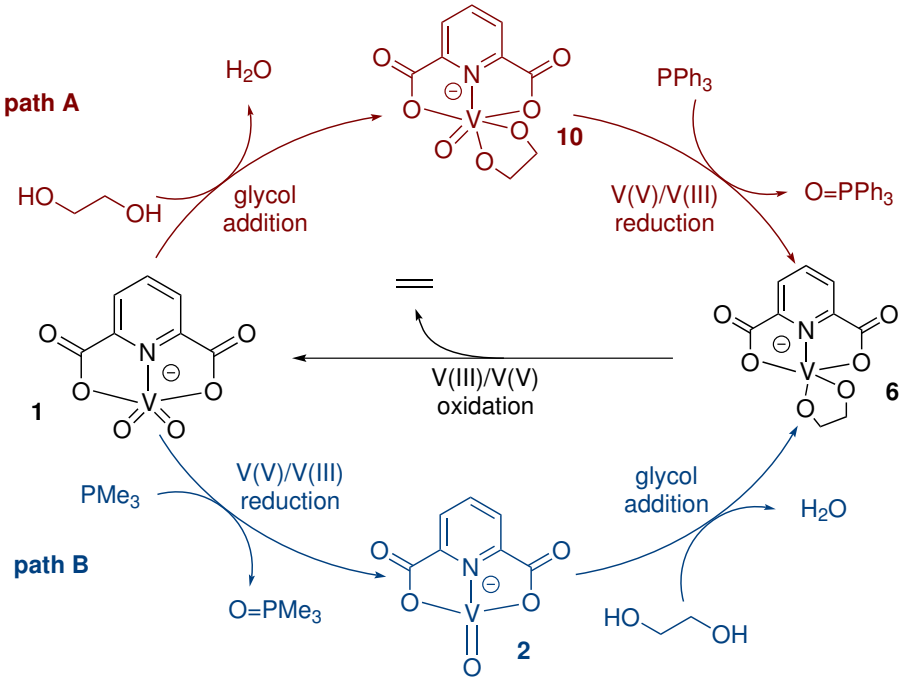


Figure 1: Mechanism of the deoxydehydration of glycols proposed by Nicholas and Chapman[20] and Galindo.[25] In path A (red), the glycol is first condensed with the V(V) complex **1**, from which an oxygen atom is then transferred to a phosphine, affording V(III) complex **6**. In path B (blue) the sequence of these steps is reversed. Both mechanisms converge in **6**, which leads to the alkene product through a concerted [3+2] retrocycloaddition.

We decided to organize our analysis of this mechanism using these two generic paths as a scaffold, although this scheme proved to be greatly oversimplified. While preparing this report, a very recent DFT study of this same reaction by Galindo came to our attention.[25] A number of his conclusions are similar to ours, however we find relevant differences in fundamental parts of the mechanism. Galindo uses single point CPCM energies in benzene on gas phase B3LYP/6-311+G* geometries and frequencies to describe two reaction paths, parallel to paths A and B in Figure 1. For both paths he characterizes triplet minima and transition states when they are lower in energy than their singlet counterparts. In his discussion, path A involves bidentate coordination of ethylene glycol to **1** through the sequential formation of a V–O bond and loss of hydrogen to an oxo group that becomes a loosely attached water molecule. The resultant hexacoordinate V(V) compound **10** is

reduced through oxygen transfer to a phosphine molecule, leading to V(III) complex **6**. This path visits the triplet potential energy surface only between the intermediate [V]–O–$PPh_3$ species that precedes the formation of **6** and **6** itself. In path B, the oxygen transfer between **1** and phosphine is the first step, leading to V(III) complex **2**. Glycol addition then leads to **6**. This path proceeds on the triplet potential energy surface between the [V]–O–$PPh_3$ species preceding the formation of **2** and **6**. The evolution of **6** to the alkene product and regeneration of the catalyst, common to both paths, is considered to proceed through an asynchronous concerted [3+2] retrocycloaddition. Galindo has found in his study that path B is globally lower in energy than path A, with the highest energy barrier in the mechanism corresponding to the alkene extrusion (**6** $\rightarrow$ **1**) with an energy of 40.2 kcal/mol relative to the reactants.[26]

In our analysis of this reaction we find that the mechanism shows significant differences when taking into account solution-phase optimized structures. Moreover, our exploration indicates that the singlet and triplet regions are not as clear cut, with a greater deal of surface hopping, and that the consideration of (di)radical species is key in the formation of the alkene and oxygen transfer processes. The characterization of the minimum energy crossing points (MECPs) between the singlet and triplet surfaces provides interesting information on the spin-crossing events, not addressed in the previous work. In studying these diradical processes, we discover a mechanism in which the formation of a vanadium metallacycle is a key step for the formation of the alkene product from the V(III) complex, which contrasts heavily with the conventionally accepted concerted retrocycloaddition step. With the description of this alternative, the activation barrier of this reaction is significantly lowered, and new possibilities for exploiting these findings through design of better catalysts are opened.

# Computational Methods

We have used Density Functional Theory in the Kohn-Sham formulation to optimize the stationary points depicted in Figures 2 and 6. The unrestricted form of the B3PW91 functional (UB3PW91)[27,28] has been used together with the Def2-TZVPP basis set.[29,30] The effect of solvation has been included in all calculations using an implicit model for benzene (PCM with the integral equation formalism variant, IEFPCM[31–33] with UAKS radii). All stationary points have been characterized as minima or transition states through harmonic analysis, and IRC calculations[34] have been used to unambiguously connect transition states to the corresponding reactants and products when needed. All this calculations have been carried out with the Gaussian09 suite of programs.[35] Bond orders and atomic charges were calculated with the Natural Bond Orbital (NBO) method, with the NBO3.1 program.[36,37]

One of the main problems that we have had to deal with during this research is the dirradical character of a significant number of species in the singlet spin potential energy surface. This led to problems with the stability of wavefunctions, due to the mixing with the triplet state, and prompted us to analyze the reaction in both the singlet and triplet potential energy surfaces. This is not an uncommon problem when dealing with structures with diradical character. The Cope reaction is a good example of this phenomenon, where the contribution of diradical components is large at the transition state.[38–40] Another recent example of the importance of taking into account the dirradical character of relevant transition structures along a mechanism is provided by the study of the isomerization of vinyl allene oxides.[41,42] The need to check the stability of wavefunctions so that we make sure that it is a real minimum in the function space is as relevant as the more widely recognized need to calculate the hessian with respect to the coordinates to characterize stationary points as minima or transition states.[43] Thus, for all stationary points the stability of the wavefunction has been computed[44] to guarantee that the wavefunctions are minima in the configuration space of the basis used.

For the location of Minimum Energy Crossing Points (MECPs) between the singlet and

triplet surfaces, we have used the method described by Harvey,[45] as implemented in the Orca program,[46] using tight convergence criteria and numerical frequencies to ensure that the crossing point found is indeed a minimum. The functional and basis set are the same used all along this work, but we have used COSMO[47] for the simulation of the effect of solvent. These MECPs, as the minima in the seams between surfaces, provide just an estimation of the region where the surface-hopping takes place and the energy needed to reach it, and thus, of the accesibility of the crossing and the feasibility of the mechanism. Evaluation of the probability of the surface hopping using spin-orbit coupling calculations should be made if more accurate kinetic information were needed about these steps in the mechanism. The high computational cost of these calculations for a system with such a large number of electrons involved in the key bond formation/breaking processes, precludes their use in this problem.

In order to save computational resources and simplify the potential energy surfaces, thus facilitating geometry optimizations, we have introduced some truncations in the model system. The first is using trimethylphosphine instead of triphenylphosphine as a reductant. The second is to use ethyleneglycol instead of glycerol, both reducing the number of electrons in the system and the potential complexity of the mechanism in terms of conformations and alternative paths that could lead to regioselectivity. The last aproximation is to use just one water molecule in mediating proton relays when such mechanisms have been considered.

# Results and Discussion

As originally proposed by Chapman and Nicholas[20] and confirmed by Galindo,[25] two are the main paths that can be proposed for this transformation, depending on the sequence in which the reduction, glycol coordination and formation of the alkene steps take place (see Figure 1). In order to facilitate the presentation and discussion of results, we will follow the same naming convention for the two paths, but we find it more convenient to start with the

description of path B.

## Path B

In this path a reduction from V(V) complex **1** to V(III) complex **2** through an oxygen transfer to a phosphine is generally proposed. This is a step common to other redox catalytic cycles involving transition metals in high oxidation states, such as rhenium or molybdenum,[48–50] but we found that this description is oversimplified and the mechanism is much more complex than what is often assumed and cannot be described as in Figure 1. The main difficulty arises from the fact that **1** is clearly a singlet (the triplet lies 73.6 kcal/mol higher in energy) and **2** a triplet (the singlet lies 6.2 kcal/mol higher in energy). Actually not only there is a crossing between the singlet and triplet surfaces between these two points, but also that the two surfaces become quite close in the whole area, leading to a very strong multirreference character of the transition states and intermediates found for this reaction. We propose two different paths for this step, which are depicted in Figure 2.

The lowest energy alternative, which corresponds to the mechanism described by Galindo (with a barrier of 34.7 kcal/mol) is a stepwise process that generates intermediate **4** through **ts1-4** associated to an activation barrier of 30.5 kcal/mol. We were not able to optimize this transition state as a stationary point on the triplet PES, but at this geometry the triplet is 4.1 kcal/mol higher in electronic energy than the singlet. Intermediate **4**, however is already more stable in the triplet state, although the difference between singlet and triplet is just 1.3 kcal/mol. Once at this point, it is worth comparing the geometries of structures **ts1-4**, **4** and the MECP, whose key features (bond distances and NBO bond orders) have been summarized in Table 1.

We find that in going from **1** to **ts1-4**, the vanadium-oxygen distance is significantly elongated by 0.276 Å, associated with a dramatic decrease in the bond order, from 2.1 to 0.77. At the same time a new phosphorous-oxygen bond is being formed, at a P–O distance of 1.66 Å and a bond order of 0.72. This transition state is considerably more advanced

Table 1: NBO bond orders and bond distances (in Å) of key structures in the oxygen transfer reaction in path B. A "t" on the name of the structure indicates the stationary point optimized on the triplet surface, while a "s" denotes the corresponding singlet.

| | V–O | | O–P | |
|---|---|---|---|---|
| structure | dist. | bond ord. | dist. | bond ord. |
| **1s** | 1.590 | 2.122 | – | – |
| **ts1-4s** | 1.866 | 0.772 | 1.655 | 0.723 |
| **4s** | 2.037 | 0.466 | 1.514 | 1.018 |
| **4t** | 2.043 | 0.458 | 1.514 | 1.020 |
| **ts4-5t** | 2.175 | 0.349 | 1.506 | 1.060 |
| **O=PMe$_3$** | – | – | 1.487 | 1.216 |
| **MECP1-4** | 1.867 | – | 1.671 | – |

than that found by Galindo, with a V–O distance of 1.78 Å and a P–O distance of 1.76 Å.[51] At the end of this step (structure **4**), the V–O bond is further debilitated at 2.04 Å and a bond order of just 0.47, while there is already a strong P–O bond in place, at 1.51 Å and 1.02 bond order. These values indicate that the structure of **4** is close to that of a phosphine oxide coordinated to vanadium, since the P–O bond is only slightly shorter in the free O=PMe$_3$, at 1.49 Å and a bond order of 1.22. There is a strong dirradical character in this structure, both as a singlet and as a triplet. One unpaired electron is localized on the vanadium center, while the second is mainly delocalized over the pyridine ring and on the oxo oxygen (see Figure 3). Thus, this step can be described as the attack of the lone pair on the phosphine to the $\pi^*_{V-O}$, so that in **4** the phosphorous atom displays positive charge (0.63 a.u. vs. 0.07 in free PMe$_3$), the V–O double bond disappears and the bonding between V and N is enhanced with respect to the values found in **1** (the V–N distance and bond order go from 2.14 to 1.94 Å and 0.45 to 0.72, respectively). With the data in Table 1 we also confirm that the triplet and singlet surfaces are very close in the region of **4**, since not only the difference in energy between **4s** and **4t** is very small, but also the geometries and bonding patterns of these two stationary points are very close.

Although there are no experimental geometries available for these structures, we have used data from similar systems to support our discussion. The V–O distance corresponding

to the metal-phosphine oxide bond in **4** is 2.04 Å, similar to the 2.00 Å in $VCl_3(OPEt_3)_3$ or the 2.08 Å in $VCl_3(THF)_3$, both V(III) complexes.[52] If we want to compare those with the distance in a vanadium oxo complex, the closest structure we found is a V(IV) complex, $[VO(acac)_2OPPh_3]$, where the V–O distance is considerably larger at 2.26 Å.[53] In both cases, the P–O bond is slightly shorter than the 1.51 Å in **4**, at 1.46/1.48 Å ($VCl_3(OPEt_3)_3$ ) or 1.49 Å ($V(C_5H_7O_2)_2O(C_{18}H_{15}OP)$). The 0.47 bond order and short V–O distances found in **4** anticipate that the departure of the phosphine oxide ligand is not trivial in this case, and all attempts to locate a transition state corresponding to this process failed. A set of constrained optimizations at different values of the V–$O_P$ bond (see SI), showed that the energy rises steadily upon the ligand departure. These results suggest that a dissociative pathway from **4** to **2** is unfavourable. Thus, an associated mechanism was explored where the the attack of a new ligand onto the vanadium center assists to expell the phosphine oxide from the coordination sphere of the metal center (**ts4-5** in Figure 2).[54]

In the second pathway, if phosphine acts as a nucleophile on the vanadium center instead of attacking the $\pi^*_{V-O}$, we can find a route connecting **1** and **2**. The coordination of a phosphine to vanadium on **1** through **ts1-3** displaces one of the carboxylate ligands of the picolinate in an $S_N2$ mechanism on the metal center. The activation barrier, of 28.8 kcal/mol is slightly lower than those corresponding to the other mechanism. Intermediate **3**, still clearly on the singlet surface (the triplet is 52.3 kcal/mol more energetic), proceeds then to **2** through a high energy transition state **ts3-2** (40.4 kcal/mol, corresponding to an activation barrier of 14.2 kcal/mol) that combines a reductive elimination of phosphine oxide with the coordination to vanadium of the previously detached carboxylate ligand.[55] Although interesting from a mechanistic point of view, this path is not competitive with the outer-sphere oxygen transfer path that avoids the formation of the V(III) complex **2**

The crossing between the singlet and the triplet energy surfaces would take place just before **2** in the inner-sphere (**ts1-3**–**3**–**ts3-2**) path, and in the vicinity of **4** in the preferred mechanism. We have calculated the MECP between the singlet and triplet surfaces in the

latter path (**MECP1-4**), finding, as expected, a structure very close in energy (1.7 kcal/mol higher) and geometry to **ts1-4**, as can be seen from the data in Table 1.

Irrespective of whether the oxygen transfer mechanism leads to **2** or **4**, the coordination of the first oxygen of the glycol proceeds, as described by Galindo, on the triplet surface, *anti* to the nitrogen, with the concerted transfer of the alcohol proton to the oxo group. We proposed a proton relay mechanism mediated by one water molecule, which can serve as a proxy of water in the reactive mixture (the alcohols obtained by processing of biomass are often mixed with some water) or another glycol molecule. We found that this relay leads to a lowering of the reaction barrier by 3.4 kcal/mol in the case of **ts2-5** and a raising of it by 0.9 kcal/mol in **ts4-5**. In **ts4-5**, it is the increase in coordination of vanadium upon complexation of the alcohol that leads to the expulsion of the phosphine oxide.

All pathways in the generic **Path B** thus converge in **5**, which evolves through a second concerted V–O coordination and proton jump, now made slightly easier (7.0 vs. 8.6 kcal/mol barrier in the non-water-mediated mechanism or 3.3 vs. 5.2 kcal/mol in the water-mediated one) thanks to a longer V–O distance in the former oxo group (2.07 Å in **ts5-6t** vs. 1.72 Å in **ts2-5t**) that allows an earlier transition state (V–$O_{glycol}$ distance of 2.18 vs. 2.10 Å).

In **ts5-6** the departure of the newly created water ligand is concerted with the proton jump and the formation of the new V–O bond, leading to V(III) complex **6**, which is more stable on the triplet surface than on the singlet, by 10.4 kcal/mol. A proton relay mechanism involving one water molecule reduces the barrier for this step by 3.7 kcal/mol.

Here is the point where our mechanistic proposal drastically differs from that of Galindo. While he proposes a concerted [3+2] retrocycloaddition singlet transition state for the formation of the alkene from **6**, with a barrier of 45.1 kcal/mol (40.2 kcal/mol over the reference of energies) we find that the reaction proceeds through a radical mechanism instead. In Figure 4 we show three dimensional structures of the main stationary points discussed in this section, including key geometric parameters.

The V(III) intermediate **6**, significantly more stable as a triplet, can evolve through

either the singlet or the triplet potential energy surfaces. In the first case, we find **ts6-1**, a concerted transition state that directly leads to the ethylene and recovery of the V(V) catalyst **1**. The barrier associated to this path is 46.1 kcal/mol (with a free energy 24.6 kcal/mol over the reference), similar to that found by Galindo. As **ts6-1** has been found as a stationary point only on the singlet potential energy surface, we have looked for the MECP between the singlet and triplet surfaces in the region between **6** and **ts6-1**. We have found that the structure of **MECP6-1** is very close to that of **6**, with V–O bonds sligthly shorter and C–O bonds slightly larger (see Table 1). The high activation energy of this transition state (**ts6-1**), and the associated antiaromatic character, as determined by a NICS(0) value of 9.1 ppm, (see Figure 7) made us to look for an alternative path.

This alternative path involves transition state **ts6-7**, still on the triplet surface, where only one of the C–O bonds is being broken, leading to the dirradical structure **7**. Although the barrier corresponding to this reaction is quite high, at 34.1 kcal/mol, **ts6-7** is only 12.5 kcal/mol more energetic than the reference, making it quite accesible. The difference of 12 kcal/mol and the avoidance of a spin-crossing event, clearly marks this as the preferred path.

The crossing between the triplet and singlet surfaces is expected to be in the region around **7**, since the singlet and triplet dirradicals are very close in energy (the singlet is only 0.3 kcal/mol more energetic than the triplet). In fact, **MECP7-8** displays a geometry very close to that of **7**, with just a slight shortening of the remaining V–O bond (by less than 0.02 Å) and a lengthening of the remaining C–O bond (by 0.04 Å). The energy of this point is just 0.7 kcal/mol higher than that of **7**.

A second transition state, still on the triplet surface (**ts7-1**), directly transforms **7** into ethylene and **1** by breaking the remaining C–O bond through a barrier of 32.7 kcal/mol. As a result, we could consider that the asynchronicity of the concerted transition state found on the singlet PES (**ts6-1**) becomes a stepwise path on the triplet PES: first breaking the longer C–O bond and afterwards breaking the remaining C–O bond after the formation of a diradical intermediate. Conversely, we could consider that the two transition structures

found on the triplet PES coalesce into just one (the asynchronicity would be a reflection of this hidden second TS) when on the singlet PES.

In this context the difference in energy between the two mechanisms is not significant, with **ts7-1** being just 2.1 kcal/mol higher in energy than **ts6-1**, although the concerted path would be slightly preferred. However, we propose a third mechanism that results in a much lower barrier for the formation of the product (15.6 kcal/mol lower than **ts7-1**).

Once intermediate **7** has been formed (**ts6-7** is 12.1 kcal/mol more stable than the alternative **ts6-1**), a rotation of the remaining O–C bond, makes this dirradical collapse to the metallacycle **8** in the singlet surface (the closed structure does not correspond to a minimum in the triplet surface). There are two isomers of this structure, depending on whether the carbon (**8-b**) or the oxygen (**8**) are *trans* to the nitrogen in this octahedral complex. The former is more stable than the latter by 6.7 kcal/mol, as expected from the *trans* series, an effect that is also reflected in the difference in the barriers for the alkene formation from these two metallacycles through a [2+2] retrocycloaddition reaction. Oxo groups, as strong $\sigma$ and $\pi$ donors have one of the strongest structural trans effects in octahedral complexes,[56] and an $R^-$ ligand, as a better $\sigma$ donor usually displays a stronger trans effect than a $OH^-$. Thus, **8-b**, with the V–C bond avoiding the coordination site *trans* to the oxo group, is more stable than its isomer **8**. The labilization of the site *trans* to the oxo group, makes **ts8-1**, in which the breaking V–C bond occupies this position, more favorable than **ts8-1-b**, in which a new oxo group is being generated at this site (the geometry at the latter transition state is quite distorted to avoid two oxo groups *trans* to each other). Thus, we propose that the reaction proceeds from **7** to **8** and then through a very low barrier of 2.7 kcal/mol **ts8-1** to the final product and the original V(V) catalyst. The formation of the more stable intermediate **8-b**, although faster than the formation of its isomer, would be a dead end, reverting to **7** instead of crossing the 16.2 kcal/mol barrier to the final product.

Looking at the free energy profile of this mechanism (See Figure 5), we identify the oxygen transfer between **1** and phosphine with a barrier of 30.5 kcal/mol, and lying 30.5 kcal/mol

Table 2: NBO bond orders and bond distances (in Å) of key structures in the alkene formation steps in path B. A "t" on the name of the structure indicates the stationary point optimized on the triplet surface, while a "s" denotes the corresponding singlet.

| | V–$O_1$ | | V–$O_2$ | | C–$O_1$ | | C–$O_2$ | | C-C | |
|---|---|---|---|---|---|---|---|---|---|---|
| structure | dist. | b.o. | dist. | b. o. | dist. | b. o. | dist. | b. o. | dist. | b. o. |
| **6t** | 1.885 | 0.559 | 1.876 | 0.838 | 1.405 | 0.951 | 1.405 | 0.943 | 1.523 | 0.995 |
| **ts6-1s** | 1.645 | 1.810 | 1.736 | 1.308 | 2.006 | 0.420 | 1.578 | 0.740 | 1.436 | 1.223 |
| **ts6-7t** | 1.643 | 1.802 | 1.897 | 0.735 | 2.061 | 0.312 | 1.403 | 0.989 | 1.487 | 1.061 |
| **7s** | 1.589 | 2.195 | 1.855 | 0.858 | — | — | 1.394 | 0.995 | 1.483 | 1.070 |
| **7t** | 1.589 | 2.195 | 1.855 | 0.858 | — | — | 1.394 | 0.995 | 1.483 | 1.070 |
| **ts7-1t** | 1.583 | 2.226 | 1.887 | 0.861 | — | — | 2.235 | 0.168 | 1.342 | 1.810 |
| **8s** | 1.608 | 2.221 | 1.765 | 1.262 | — | — | 1.472 | 0.818 | 1.495 | 1.072 |
| **8bs** | 1.583 | 2.265 | 1.985 | 0.946 | — | — | 1.411 | 0.966 | 1.499 | 1.031 |
| **ts8-1s** | 1.600 | 2.174 | 1.703 | 1.517 | — | — | 1.710 | 0.540 | 1.421 | 1.304 |
| **ts8-1bs** | 1.578 | 2.239 | 1.682 | 1.567 | — | — | 1.821 | 0.450 | 1.417 | 1.310 |
| **C=C** | — | — | — | — | — | — | — | — | 1.324 | 2.050 |
| **MECP6-1** | 1.871 | — | 1.867 | — | 1.406 | — | 1.409 | — | 1.523 | — |
| **MECP7-8** | 1.590 | — | 1.836 | — | — | — | 1.437 | — | 1.476 | — |

over the separated reactants in energy as a potential rate-limiting step. In contrast, the strength of the P–O bond in phosphine oxide, makes **ts6-7t** and **ts8-1** at 12.5 and 11.1 kcal/mol, respectively lower in energy than the reactants, although the activation barrier for the first C–O bond breaking is larger than for the oxygen transfer, at 34.1 kcal/mol. To elucidate which barrier is going to affect the kinetics of the reaction the most, something needed to devise ways to improve the catalyst, we have applied the energetic span model[57,58] to the radical mechanism we propose as preferred for this transformation: **1**–**4t**–**5t**–**6t**–**7t**–**8**–**1** We have neglected any assumption about the probability of the surface hops, and used the lowest energy structure (be it either in the triplet or the singlet potential energy surface) for every minimum or transition state along the path. As a result, all spin-crossings along the mechanism are considered to proceed without any kind of energy penalty or delay. In this framework, the TOF-determining transition state is found to be **ts6-7**, with **6** as the TOF-determining intermediate. Transition state **ts8-1** has a non-negligeable influence on the TOF (turn-over frequency) as well, with a contribution of 0.16 (vs. 0.82 for **ts6-7**). Thus the

concept of turn-over determining step in this mechanism could be applied to the homolytic breaking of the C–O bond in **6**. Using 160°C as the working temperature (the experimental work by Chapman *et al.*[20] report a 150-170°C interval), the TOF for this reaction is found to be $3.8 \cdot 10^{-5} s^{-1}$ and the energetic span of the reaction 34.1 kcal/mol. Application of this kinetic model to the alternative going through a concerted transition state for the formation of the alkene: **1**–**4t**–**5t**–**6t**–**1**, which agrees with the proposal by Galindo,[25] leds to a much lower TOF ( $3.7 \cdot 10^{-12} s^{-1}$) and higher energetic span (46.2 kcal/mol), making the radical mechanism the preferred reaction path. The stepwise mechanism not involving the formation of the metallacycle (going through **ts7-1**) is even less favourable than the concerted path, with a TOF of $3.3 \cdot 10^{-12} s^{-1}$ and a energetic span of 48.3 kcal/mol. In all three cases, the potential well associated to the stability of the pair **6** + phosphine oxide with respect to **1**, phosphine and the free glycol, makes the oxygen transfer between the V(V) catalyst and the phosphine reductant not kinetically relevant, and **ts6-7**, **ts6-1** or **ts7-1** become the turn-over frequency dermining steps of the considered mechanisms.

As a proof of concept of the possibilities that such a mechanistic analysis can open for the design of improved catalysts, we explore two simple ways of lowering the considerably high activation barriers of the reaction. First, we propose one structural modification of the glycol that would stabilize the dirradical in **7**, thus facilitating the breaking of the first C–O bond in this step of the mechanism. Adding two methyl substituents on the carbon supporting the radical, lowers the barrier of this step by 3.7 kcal/mol (the barrier is 30.4 kcal/mol), and further differentiates this TS from the concerted alternative (**ts6-1**) lying 15.3 kcal/mol higher in energy. As a result, it is expected that this reaction will be more favorable with longer diol chains, more interesting substrates, from an industrial point of view, than the simple model used in this paper.

This success prompted us to propose a modification of the catalyst that would stabilize the radical on the metal center, which would be a first step in the design of a better catalyst for this transformation. Replacement of the oxygens coordinated to vanadium in the dipicolinate

ligand by sulfur atoms, known to stabilize radicals on transition metal complexes[59] led to a barrier of just 23.0 kcal/mol for triplet **ts6-7**, the rate determining step in the mechanism. The concerted alternative on the singlet surface (**ts6-1**) is no longer a transition state in this system, and becomes a second order saddle point 14.6 kcal/mol higher in energy than **ts6-7**. Calculation of **ts1-4**, which can take over as the rate-determining step for this sulfur-substituted system if the barrier associated to **ts6-7** is lowered, led us to a barrier of 27.1 kcal/mol for the most costly step in the oxygen transfer between vanadium and phosphine, also reduced with respect to the barrier corresponding to the parent system (30.5 kcal/mol).

Thus, replacing the oxygen atoms on the vanadium catalyst by sulfurs could be a good way of experimentally testing the soundness of our mechanistic proposal. Other alternatives could involve the use of radical scavengers that would hinder the formation or evolution of intermediate **7**.

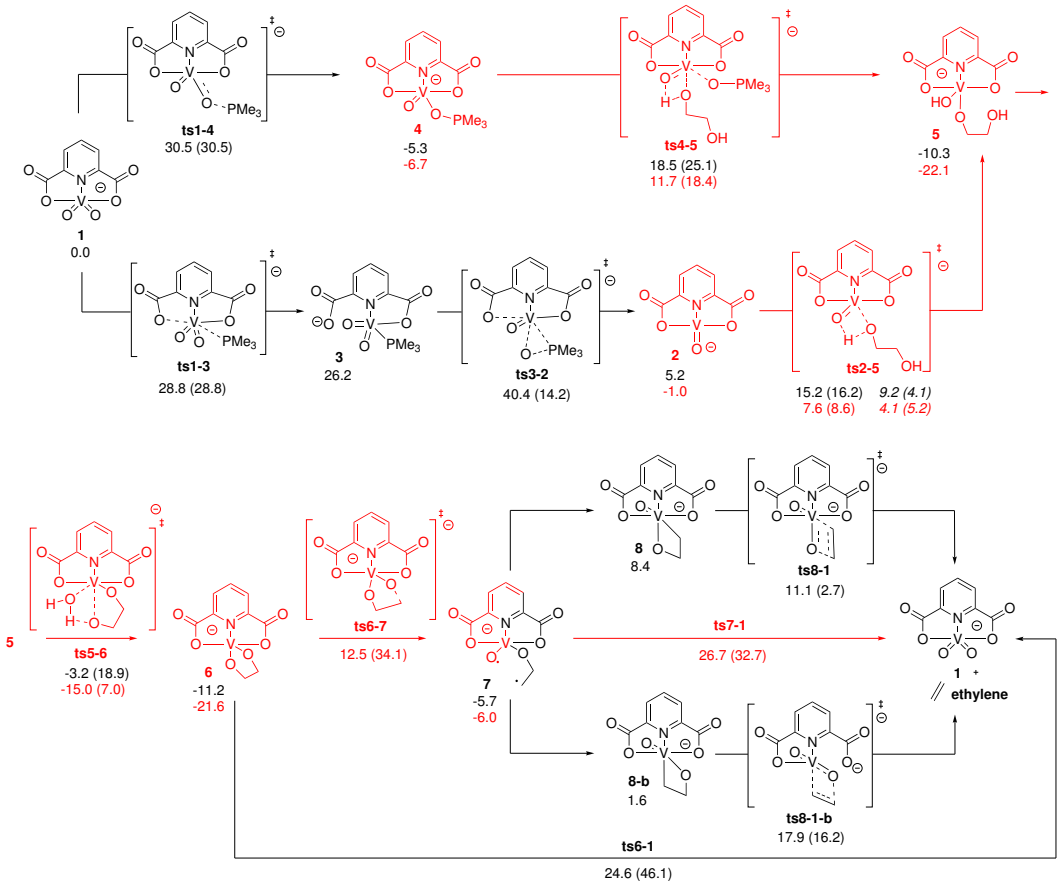


Figure 2: Proposed mechanisms for path B. Most structures depicted have been calculated in both the triplet (energies in red) and singlet (in black) potential energy surfaces. Gibbs free energies (all values are in kcal/mol) are provided with respect to singlet **1**, ethyleneglycol, water and phosphine. Activation free energies (in parentheses) are calculated with respect to the previous lowest energy minima, irrespective of their spin state. The structures colored in red are those for which the most stable spin state is the triplet. In the case of **7** a mix of colors has been used to make it clear that for this dirradical, singlet and triplet states are almost degenerate.

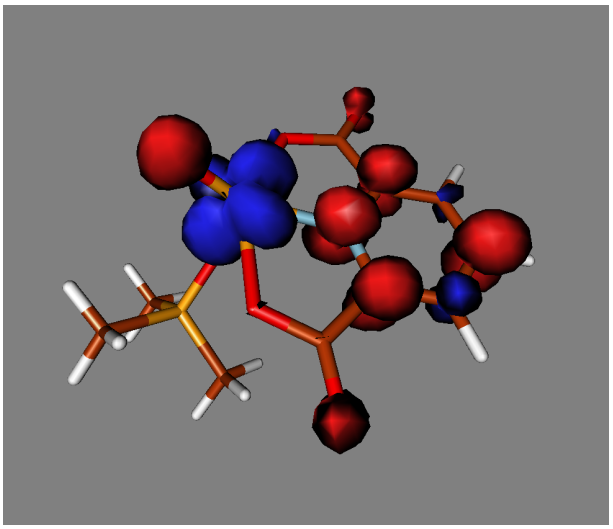

Figure 3: Spin density for **4** in the singlet state (isosurface at 0.005 au).

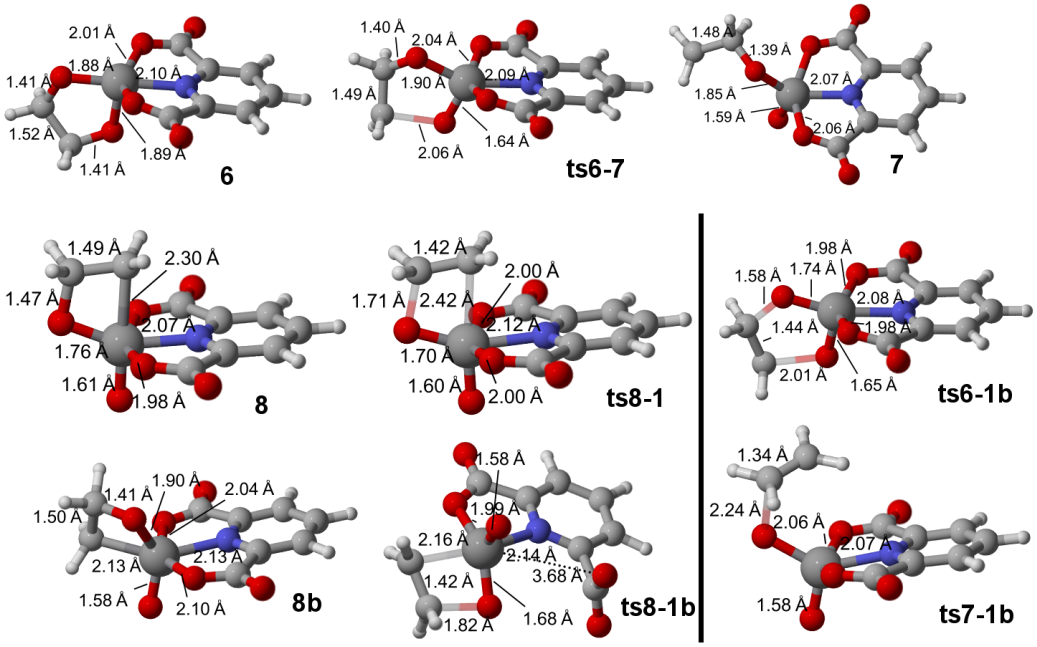


Figure 4: Three dimensional representation of the key stationary points in the proposed radical mechanism. The key transition state in the concerted path proposed by Galindo, **ts6-1** and **ts7-1** have also been included for comparison. Relevant bond distances (in Å) are displayed on the structures.

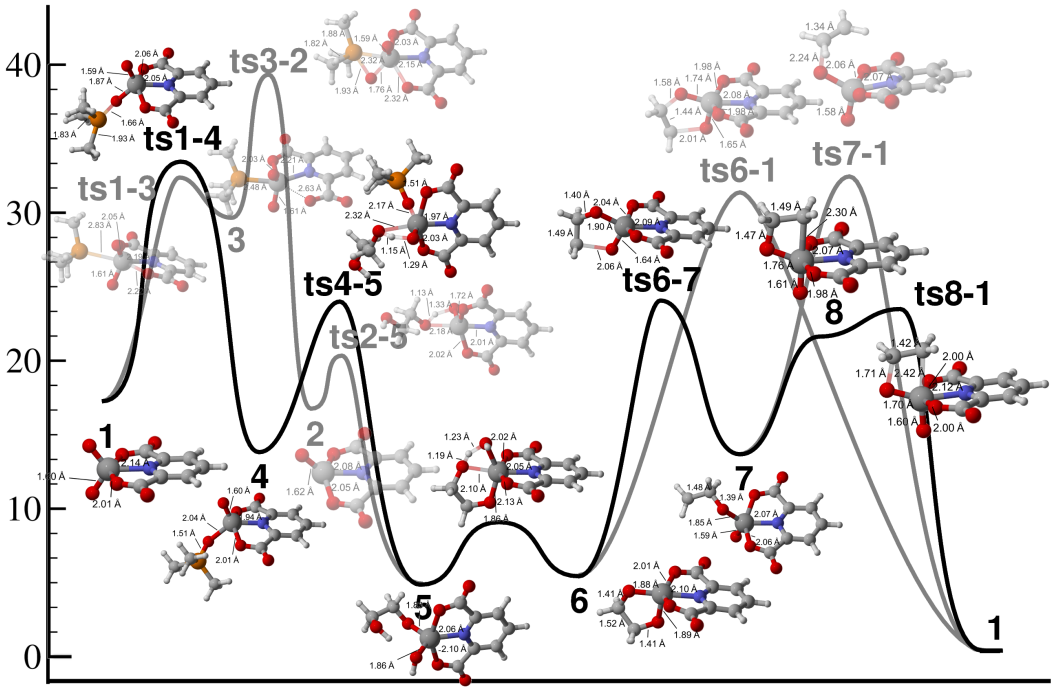


Figure 5: Proposed reaction profile for the preferred path B (in black). Transparency and grey is used to display the higher energy alternatives to different sections of the main path. Free energy values are in kcal/mol. 3D representations of the stationary points along the path (those on the preferred PES), where some key bond distances are highlighted, have been included for clarity.

## Path A

This path starts with the condensation of the glycol on the V(V) catalyst **1** (see Figure 6). The mechanism for this condensation is analogous to that described by Galindo: a first concerted transition state where the V–O bond is formed at the same time the proton jumps from the alcohol to one of the oxo groups on the metal center. Two trajectories have been analyzed for the attack of the alcohol, both resulting in the formation of an octahedral complex: 1) perpendicular to the chelate ligand plane, and *trans* to an oxo group, so that the oxo group receiving the proton is *trans* to the nitrogen (**ts1-9**), and 2) *trans* to the nitrogen, so that the oxo receiving the proton is perpendicular to the plane of the chelate (**ts1-9-b**). In this second case, some conformations can generate a hydrogen bond between the non-reacting hydroxyl group of the glycol and the second oxo ligand on vanadium, but the extra stabilization provided by this hydrogen bond does not compensate the penalty of attacking *trans* to the nitrogen, and the lowest barrier found is still 8.9 kcal/mol larger than the 26.9 kcal/mol corresponding to **ts1-9**. This step leads to hexacoordinated complex **9**, lying 24.0 kcal/mol higher in energy than the separated reactants (See Supporting Information for the structures).

The coordination of the second hydroxy group to the vanadium proceeds via a similar transition state where the V–O bond formation, proton transfer and departure of the newly formed water molecule happen in concert. We were not able to locate a minimum in the potential energy surface where water is coordinated to **10**, the product of this step. Surprisingly, the invocation of a proton relay mechanism involving one water molecule does not lower the barrier of this step, but makes it larger instead (18.7 kcal/mol). In parallel to what we observed in **Path B**, the barrier for this V–O bond formation is lower than the first (12.3 vs. 26.9 kcal/mol, although this is attribuable to the instability of intermediate **9**, 24.0 kcal/mol higher in energy than the separate reactants). Intermediate **10** is more stable than **9**, at 12.6 kcal/mol, probably due to a chelate effect.

Once the condensation of the glycol on the V(V) complex has been achieved, this V(V)

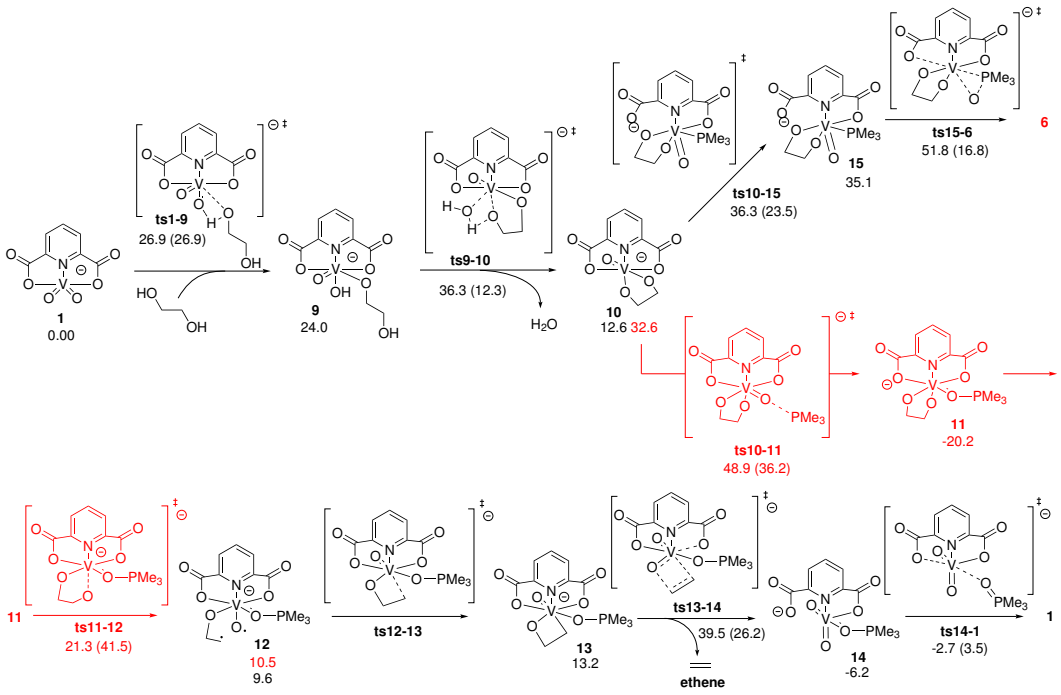


Figure 6: Proposed mechanisms for path A. Most structures depicted have been calculated in both the triplet (energies in red) and singlet (in black) potential energy surfaces. Gibbs free energies (all values are in kcal/mol) are provided with respect to singlet **1**, ethyleneglycol, water and phosphine. Activation free energies (in parentheses) are calculated with respect to the previous lowest energy minima, irrespective of their spin state. The structures colored in red are those for which the most stable spin state is the triplet.

center needs to be reduced to V(III). The proposed mechanism is an oxygen transfer reaction, similar to that found for **1** in **Path B** (see Figures 2 and 6). Thus, we can find two alternative paths for the reduction of V(V) to V(III).

The first, involves a nucleophilic attack of the phosphine to the vanadium center, displacing a carboxylate from the metal and leading to hexacoordinated complex **15** through transition state **ts10-15**. The activation barrier associated to this process is rather high, at 23.6 kcal/mol, and the resultant intermediate is only 1.3 kcal/mol more stable than this TS. The evolution of this intermediate **15** through a reductive elimination and re-attachment of the dangling carboxylate to **6**, where the mechanism would converge to that shown in **Path B**, involves another high energy step (a barrier of 16.8 kcal/mol and a TS 51.8 kcal/mol over the energy reference). As found in **Path B**, this inner-sphere mechanism on a vanadium

center is not the most favored way of effecting a oxygen transfer between an oxovanadium complex and a phosphine.

The second path, involves an attack of the phosphine to the oxo group on the vanadium center. Triplet and singlet are close in this region, but the transition state (**ts10-11**) is lower in energy on the triplet surface, with a barrier of 36.2 kcal/mol, corresponding to a free energy of 48.9 kcal/mol relative to the reactants. As did Galindo, we find that this first step in the oxygen transfer between vanadium and phosphine is the rate limiting step in **Path A**, making **Path B** the preferred alternative for the studied vanadium-catalyzed deoxydehydration of glycols. This transition state would lead to hexacoordinated intermediate **11** on the triplet surface, with a relative free energy of -20.2 kcal/mol.

Despite not being competitive, this path is worth studying, since it provides interesting information on the effect of the coordination number and oxidation state of the metal on the reactions involved in the oxygen transfer between vanadium and phosphorous and on the alkene extrussion. Again on complex **11**, as we did on **4**, we find that the cleavage of phosphine oxide from vanadium is not trivial (we were not able to locate a transition state for this reaction, and the energy continuously rises as the V–O distance increases. As a result, although the mechanism for the alkene extrussion is similar in paths A and B, these two paths don't converge in structure **6**, as proposed by Galindo.

After **11**, one of the C–O bonds is cleaved through **ts11-12**, to provide diradical triplet **12**. In this step O=$PPMe_3$ is still coordinated to the vanadium center. We have found that the cleavage of the C–O bond *anti* to the nitrogen is slightly preferred (0.2 kcal/mol) to the cleavage of the C–O bond *anti* to the phosphine oxide, but the two branches of the path thus opened readily converge as the resultant diradical collapses to metallacycle **13** through a transition state (**ts12-13**) with an activation barrier of 10.8 kcal/mol.[60] Intermediate **13** evolves then through **ts13-14** to the alkene and the V(V) compound **14**. And it is only on the last step of the reaction (**ts14-1**), after the alkene has been formed, that the nucleophilic attack of the dangling carboxylate displaces the phosphine oxide ligand from the metal

center.

Interestingly, the NICS on points along a line perpendicular to the center of the C–C–O–V ring, show the strong aromatic character of **ts13-14**, which compares well to that found for **ts8-1-b** in **path B** (see Figure 7). Thus, we can describe these two steps in the mechanism as a [2+2] retrocycloadditions. These reactions, only allowed in an antara/supra approach in organic systems, can proceed through a non-twisted transition state in organometallic metallacycles, since an allowed, 4-$\pi$ electron, Möbius system is achieved through the extra node in the *d* orbital of the metal center that is forming the new V–O double bond in the product.[61]

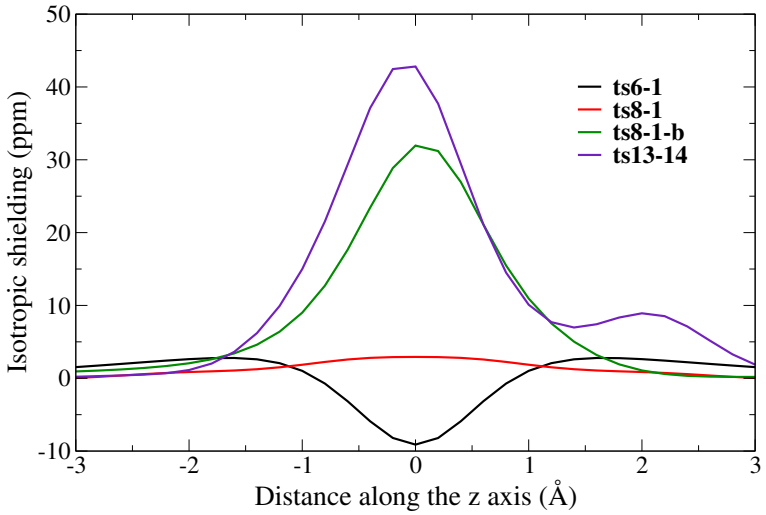


Figure 7: Isotropic shielding (ppm) vs. distance (Å) along a straight line perpendicular to the ring plane crossing its center in selected transition states along the two mechanisms.

The main difference between these two transition structures and **ts8-1** in path B, which does not display aromatic character (see Figure 7), is the permanence in the latter of the two V–O bonds to the carboxylate group of the dipicolinate ligand, instead of just one. As a result of this, there is a marked difference in the charge on vanadium, which becomes more positive, going from 0.60 and 0.65 a.u. in **ts13-14** and **ts8-1-b** to 0.39 in **ts8-1** and in the charge on the carbon attached to the metal center, wich increases from -0.32 and -0.30 in **ts13-14** and **ts8-1-b** to -0.53 in **ts8-1**. This is also reflected in the breaking C–V and C–O distances, 2.42 and 1.71 Å, respectively in **ts8-1**, and 2.16 and 1.82 Å in **ts8-1-b**, speaking

of a more asynchronous transition state in the former.

# Conclusions

In this work, we find that, as already proposed by Galindo,[25] the DODH of glycols catalyzed by a $[VO_2(dipic)]^-$ complex using a phosphine as a reducing agent proceeds through a mechanism involving the initial reduction of the V(V) catalyst to V(III) by the phosphine, followed by condensation of the glycol and further formation of the alkene product (**path B**). A reaction path where the order of the condensation and reduction steps is reversed (**path A**), has been found to be non-competitive.

In contrast with previous reports, however, we have found a stepwise alternative to the antiaromatic [3+2] concerted retrocycloaddition commonly thought to connect the V(III)-glycol complex **6** into the alkene product. This path is considerably lower in energy (by 12.1 kcal/mol) than the concerted alternative and involves the formation of diradical **7** and its collapse to a metallacycle with a direct C–V bond, which then evolves through an aromatic [2+2] retrocycloaddition, allowed by the intervention of the *d* orbitals on the metal center. We have found that the TOF-determining step of the mechanism is the cleavage of the O–C bond in **6** to form dirradical **7** and we propose as a result the use of sulfur ligands on the vanadium center as a potential improvement of the catalytic system.

We describe the mechanism of this transformation as an example of two-state reactivity, where the system travels along the singlet and triplet potential energy surfaces and have characterized the MECPs in the seams between where the two surfaces cross along the mechanism.

Together with that, we have explored alternative mechanisms to the reduction of the V(V) complex by phosphines (both before, in path B, and after, in path A, condensation of the glycol has taken place) that share interesting features that provide a better understanding of V(III)/V(V) cycles, which could be potentially exploited in the design of other oxygen transfer processes (see Figure 2).

The main results of this study are summarized in the reaction profile in Figure 5, where we have used transparency to represent higher energy alternatives to the proposed mechanism

for **path B**.

## Acknowledgement

We thank the Centro de Supercomputación de Galicia (CESGA) for the allocation of computational resources and the Xunta de Galicia and Ministerio de Economía y Competitividad for funding through projects EM2014/040 and CTQ2013-48937-C2-1-P and CTQ2013-48937-C2-2-P, respectively. MCR thanks the Ministerio de Educación Cultura y Deporte for a FPU fellowship.

## Supporting Information Available

The scan starting from **4** and the 3-D structures of **9**, **9-b**, **ts1-9** and **ts1-9-b** are available in the Supporting Information. DFT energies and cartesian coordinates for each stationary point are available in a xyz file for each structure.

This material is available free of charge via the Internet at `http://pubs.acs.org/`.

## References

(1) Nakagawa, Y.; Tamura, M.; Tomishige, K. Catalytic Materials for the Hydrogenolysis of Glycerol to 1,3-Propanediol. *J. Mater. Chem. A* **2014**, *2*, 6688–6702.

(2) Gandarias, I.; Arias, P. L.; Fernández, S. G.; Requies, J.; Doukkali, M. E.; Güemez, M. B. Hydrogenolysis Through Catalytic Transfer Hydrogenation: Glycerol Conversion to 1,2-Propanediol. *Catal. Today* **2012**, *195*, 22–31.

(3) Nakagiri, T.; Murai, M.; Takai, K. Stereospecific Deoxygenation of Aliphatic Epoxides to Alkenes under Rhenium Catalysis. *Org. Lett.* **2015**, *17*, 3346–3349.

(4) McClain II, J. M.; Nicholas, K. M. Elemental Reductants for the Deoxydehydration of Glycols. *ACS Catal.* **2014**, *4*, 2109–2112.

(5) Fernandes, T. A.; Bernardo, J. R.; Fernandes, A. C. Direct Reductive Deoxygenation of Aryl Ketones Catalyzed by Oxo-Rhenium Complexes. *ChemCatChem* **2015**, *7*, 1177–1183.

(6) Dethlefsen, J. R.; Fristrup, P. In Situ Spectroscopic Investigation of the Rhenium-Catalyzed Deoxydehydration of Vicinal Diols. *ChemCatChem* **2015**, *7*, 1184–1196.

(7) Dethlefsen, J. R.; Fristrup, P. Rhenium-Catalyzed Deoxydehydration of Diols and Polyols. *ChemSusChem* **2014**, *8*, 767–775.

(8) Raju, S.; Moret, M.-E.; Gebbink, R. J. M. K. Rhenium-Catalyzed Dehydration and Deoxydehydration of Alcohols and Polyols: Opportunities for the Formation of Olefins from Biomass. *ACS Catal.* **2015**, *5*, 281–300.

(9) Boucher-Jacobs, C.; Nicholas, K. M. Oxo-Rhenium-Catalyzed Deoxydehydration of Polyols With Hydroaromatic Reductants. *Organometallics* **2015**, *34*, 1985–1990.

(10) Kasner, G. R.; Boucher-Jacobs, C.; McClain II, J. M.; Nicholas, K. M. Oxo-Rhenium Catalyzed Reductive Coupling and Deoxygenation of Alcohols. *Chem. Commun.* **2016**, *52*, 7257–7260.

(11) Bernardo, J. R.; Fernandes, A. C. Deoxygenation of Carbonyl Compounds Using an Alcohol as an Efficient Reducing Agent Catalyzed by Oxo-Rhenium Complexes. *Green Chem.* **2016**, *18*, 2675–2681.

(12) Wu, D.; Zhang, Y.; Su, H. Mechanistic Study on Oxorhenium-Catalyzed Deoxydehydration and Allylic Alcohol Isomerization. *Chem. Asian J.* **2016**, *11*, 1565–1571.

(13) Shiramizu, M.; Toste, F. D. Expanding the Scope of Biomass-Derived Chemicals through Tandem Reactions Based on Oxorhenium-Catalyzed Deoxydehydration. *Angew. Chem. Int. Ed.* **2013**, *52*, 12905–12909.

(14) Liu, S.; Senocak, A.; Smeltz, J. L.; Yang, L.; Wegenhart, B.; Yi, J.; Kenttämaa, H. I.; Ison, E. A.; Abu-Omar, M. M. Mechanism of MTO-Catalyzed Deoxydehydration of Diols to Alkenes Using Sacrificial Alcohols. *Organometallics* **2013**, *32*, 3210–3219.

(15) Li, X.; Wu, D.; Lu, T.; Yi, G.; Su, H.; Zhang, Y. Highly Efficient Chemical Process To Convert Mucic Acid into Adipic Acid and DFT Studies of the Mechanism of the Rhenium-Catalyzed Deoxydehydration. *Angew. Chem. Int. Ed.* **2014**, *53*, 4200–4204.

(16) Coskun, T.; Conifer, C. M.; Stevenson, L. C.; Britovsek, G. J. P. Carbodeoxygenation of Biomass: The Carbonylation of Glycerol and Higher Polyols to Monocarboxylic Acids. *Chem. Eur. J.* **2013**, *19*, 6840–6844.

(17) Hills, L.; Moyano, R.; Montilla, F.; Pastor, A.; Galindo, A.; Álvarez, E.; Marchetti, F.; Pettinari, C. Dioxomolybdenum(VI) Complexes with Acylpyrazolonate Ligands: Synthesis, Structures, and Catalytic Properties. *European Journal of Inorganic Chemistry* **2013**, *2013*, 3352–3361.

(18) Garcia, N.; García-García, P.; Fernández-Rodríguez, M. A.; García, D.; Pedrosa, M. R.; Arnáiz, F. J.; Sanz, R. An Unprecedented Use for Glycerol: Chemoselective Reducing Agent for Sulfoxides. *Green Chem.* **2013**, *15*, 999–1005.

(19) García, N.; García-García, P.; Fernández-Rodríguez, M. A.; Rubio, R.; Pedrosa, M. R.; Arnáiz, F. J.; Sanz, R. Pinacol as a New Green Reducing Agent: Molybdenum- Catalyzed Chemoselective Reduction of Sulfoxides and Nitroaromatics. *Adv. Synth. Catal.* **2012**, *354*, 321–327.

(20) Chapman Jr., G.; Nicholas, K. M. Vanadium-Catalyzed Deoxydehydration of Glycols. *Chem. Commun.* **2013**, *49*, 8199–8201.

(21) Dethlefsen, J. R. and Lupp, D. and Oh, B-C. and Fristrup, P., Molybdenum-Catalyzed Deoxydehydration of Vicinal Diols. *ChemSusChem* **2014**, *7*, 425–428.

(22) Dethlefsen, J. R.; Lupp, D.; Teshome, A.; Nielsen, L. B.; Fristrup, P. Molybdenum-Catalyzed Conversion of Diols and Biomass-Derived Polyols to Alkenes Using Isopropyl Alcohol as Reductant and Solvent. *ACS Catal.* **2015**, *5*, 3638–3647.

(23) Lupp, D.; Christensen, N. J.; Dethlefsen, J. R.; Fristrup, P. DFT Study of the Molybdenum-Catalyzed Deoxydehydration of Vicinal Diols. *Chem. Eur. J.* **2015**, *21*, 3435–3442.

(24) Sousa, S. C.; Fernandes, A. C. Efficient Deoxygenation Methodologies Catalyzed by Oxo-Molybdenum and Oxo-Rhenium Complexes. *Coord. Chem. Rev.* **2015**, *284*, 67–92.

(25) Galindo, A. Dft Studies on the Mechanism of the Vanadium-Catalyzed Deoxydehydration of Diols. *Inorg. Chem.* **2016**, *55*, 2284–2289.

(26) The activation barrier corresponding to this step would be 45.1 kcal/mol or 21.4 kcal/mol, depending on whether the previous minimum is considered to be **6** on the triplet or on the singlet surface. With $PMe_3$ the relative free energy of this TS is 35.2 kcal/mol in benzene.

(27) Becke, A. D. Density functional thermochemistry. III. The role of exact exchange. *J. Chem. Phys.* **1993**, *98*, 5648–5652.

(28) Perdew, J. P.; Chevary, J. A.; Vosko, S. H.; Jackson, K. A.; Pederson, M. R.; Singh, D. J.; Fiolhais, C. Atoms, Molecules, Solids, and Surfaces: Applications of the Generalized Gradient Approximation for Exchange and Correlation. *Phys. Rev. B* **1992**, *46*, 6671–6687.

(29) Weigend, F.; Ahlrichs, R. Balanced Basis Sets of Split Valence, Triple Zeta Valence and Quadruple Zeta Valence Quality for H to Rn: Design and Assessment of Accuracy. *Phys. Chem. Chem. Phys.* **2005**, *7*, 3297–3305.

(30) Schäfer, A.; Horn, H.; Ahlrichs, R. Fully Optimized Contracted Gaussian Basis Sets for Atoms Li to Kr. *J. Chem. Phys.* **1992**, *97*, 2571–2577.

(31) Tomasi, J.; Persico, M. Molecular Interactions in Solution: An Overview of Methods Based on Continuous Distributions of the Solvent. *Chem. Rev.* **1994**, *94*, 2027–2094.

(32) Tomasi, J.; Mennucci, B.; Cammi, R. Quantum Mechanical Continuum Solvation Models. *Chem. Rev.* **2005**, *105*, 2999–3094.

(33) Cancés, E.; Mennucci, B. The Escaped Charge Problem in Solvation Continuum Models. *J. Chem. Phys.* **2001**, *115*, 6130–6135.

(34) González, C.; Schlegel, H. B. Reaction Path Following in Mass-Weighted Internal Coordinates. *J. Chem. Phys.* **1990**, *94*, 5523–5527.

(35) Frisch, M. J. et al. Gaussian09 Revision E.01. Gaussian Inc. Wallingford CT 2009.

(36) Reed, A. E.; Curtiss, L. A.; Weinhold, F. Intermolecular Interactions from a Natural Bond Orbital, Donor-Acceptor Viewpoint. *Chem. Rev.* **1988**, *88*, 899–926.

(37) Glendening, E. D.; Reed, A. E.; Carpenter, J. E.; Weinhold, F. NBO Version 3.1.

(38) Blavins, J. J.; Cooper, D. L.; Karadakov, P. B. Aromatic vs Diradical Character in the Transition States of the Cope Rearrangements of 1,5-Hexadiene and Its Cyano Derivatives. *J. Phys. Chem. A.* **2004**, *108*, 194–202.

(39) Salvatella, L. Theoretical Design of Tetra(Arenediyl)Bis(Allyl) Derivatives as Model Compounds for Cope Rearrangement Transition States. *RSC Adv.* **2015**, *5*, 11494–11497.

(40) McGuire, M. J.; Piecuch, P. Balancing Dynamic and Nondynamic Correlation for Diradical and Aromatic Transition States: A Renormalized Coupled-Cluster Study of the Cope Rearrangement of 1,5-Hexadiene. *J. Am. Chem. Soc.* **2005**, *127*, 2608–2614.

(41) López, R. V.; Faza, O. N.; López, C. S. Accounting for Diradical Character through DFT. The Case of Vinyl Allene Oxide Rearrangement. *J. Org. Chem.* **2015**, *80*, 11206–11211.

(42) Hebert, S. P.; Cha, J. K.; Brash, A. R.; Schlegel, H. B. Investigation into 9(s)-HPODE-Derived Allene Oxide to Cyclopentenone Cyclization Mechanism Via Diradical Oxyallyl Intermediates. *Org. Biomol. Chem.* **2016**, *14*, 3544–3557.

(43) Hoffmann, R.; Schleyer, P.; Schaefer, H. Predicting Molecules-More Realism, Please! *Angew. Chem. Int. Ed.* **2008**, *47*, 7164–7167.

(44) Bauernschmitt, R.; Ahlrichs, R. Stability Analysis for Solutions of the Closed Shell Kohn-Sham Equation. *J. Chem. Phys.* **1996**, *104*, 9047–9052.

(45) Poli, R.; Harvey, J. N. Spin Forbidden Chemical Reactions of Transition Metal Compounds. New Ideas and New Computational Challenges. *Chem. Soc. Rev.* **2003**, *32*, 1–8.

(46) Neese, F. The Orca Program System. *Wiley Interdiscip. Rev. Comput. Mol. Sci.* **2012**, *2*, 73–78.

(47) Klamt, A.; Schüürmann, G. COSMO: A new approach to dielectric screening in solvents with explicit expressions for the screening energy and its gradient. *J. Chem. Soc. Perkin Trans.* **1993**, *2*, 799–805.

(48) Wang, Y.; ; Espenson, J. H. Efficient Catalytic Conversion of Pyridine N-Oxides to Pyridine with an Oxorhenium(V) Catalyst. *Org. Lett.* **2000**, *2*, 3525–3526.

(49) Sanz, R.; Escribano, J.; Fernández, Y.; Aguado, R.; Pedrosa, M. R.; Arnáiz, F. J. Deoxygenation of N-Oxides with Triphenylphosphine Catalyzed by Dichlorodioxomolybdenum(VI). *Synlett* **2005**, *9*, 1389–1392.

(50) Sanz, R.; Escribano, J.; Pedrosa, M.; Aguado, R.; Arnáiz, F. Dioxomolybdenum(VI)-Catalyzed Reductive Cyclization of Nitroaromatics. Synthesis of Carbazoles and Indoles. *Adv. Synth. & Catal.* **2007**, *349*, 713–718.

(51) Any stationary point we optimized with distances around these values was found to have a unstable wavefunction.

(52) Cotton, F.; Lu, J.; Ren, T. Phosphine and Phosphine Oxide Adducts of Vanadium(Iv) Chloride: Synthesis and Structural Studies. *Inorg. Chim. Acta* **1994**, *215*, 47–54.

(53) Chen, H.; Si, Y.; Chen, C.; Liu, Q. Bis(acetylacetonato)oxido(triphenylphosphine oxide)Vanadium(IV). *Acta Crystallogr. Sect. E* **2008**, *64*, m159.

(54) The V–$O_P$ and O–P distances in **ts4-5** are 2.17 Å and 1.51 Å, respectively. We were able to follow the IRC corresponding to this TS up until they became 2.21 and 1.50 Å, respectively.

(55) **ts3-2** does not seem to be a stationary point in the triplet potential energy surface, so we calculated the energy of the triplet wavefunction corresponding to the optimized singlet geometry, obtaining a 0.9 kcal/mol singlet-triplet gap.

(56) Coe, B. J.; Glenwright, S. J. Trans-Effects in Octahedral Transition Metal Complexes. *Coord. Chem. Rev.* **2000**, *203*, 5–80.

(57) Kozuch, S.; Shaik, S. How to Conceptualize Catalytic Cycles? The Energetic Span Model. *Acc. Chem. Res.* **2011**, *44*, 101–110.

(58) Kozuch, S. A Refinement of Everyday Thinking: the Energetic Span Model for Kinetic

Assessment of Catalytic Cycles. *Wiley Interdiscip. Rev. Comput. Mol. Sci.* **2012**, *2*, 795–815.

(59) Morsing, T. J.; MacMillan, S. N.; Uebler, J. W. H.; Brock-Nannestad, T.; Bendix, J.; Lancaster, K. M. Stabilizing Coordinated Radicals via MetalLigand Covalency: A Structural, Spectroscopic, and Theoretical Investigation of Group 9 Tris(dithiolene) Complexes. *Inorg. Chem.* **2015**, *54*, 3660–3669.

(60) This barrier has been calculated with structures optimized in acetonitrile, since we could not characterize **ts12-13** in benzene.

(61) Upton, T. H.; Rappe, A. K. A Theoretical Basis for Low Barriers in Transition-Metal Complex $2\pi + 2\pi$ Reactions: the Isomerization of the Dicyclopentadienyltitanium Complex $Cp_2TiC_3H_6$ to $Cp_2TiCH_2(C_2H_4)$. *J. Am. Chem. Soc.* **1985**, *107*, 1206–1218.

# Graphical TOC Entry

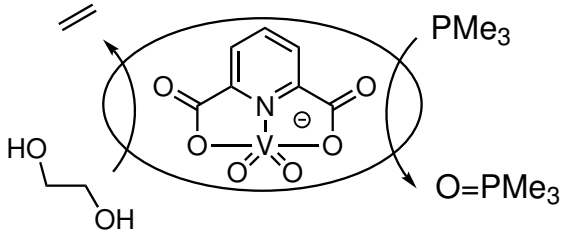


The mechanism of the $[VO_2(dipic)]^-$ catalyzed DODH of glycols using $PMe_3$ as a reductant has been shown to proceed through a radical mechanism after the initial V(V)/V(III) reduction and glycol condensation, with an energetic span 12 kcal/mol lower than that of the usually accepted concerted alternative.